Growth and Photodissociation of Cr_x−(Coronene)$_y$ Complexes

N. R. Foster, G. A. Grieves, J. W. Buchanan, N. D. Flynn, and M. A. Duncan*

Department of Chemistry, University of Georgia, Athens, Georgia 30602-2556

Received: June 12, 2000; In Final Form: September 11, 2000

Gas-phase complexes are produced containing one or more chromium atoms bound to one or more molecules of the polycyclic aromatic hydrocarbon (PAH) coronene ($C_{24}H_{12}$). These species are prepared with laser vaporization in a pulsed-nozzle cluster source of a chromium rod coated with a thin film of coronene. Mass spectroscopy reveals the formation of clusters of the form Cr_x(coronene)$_y^+$ up to sizes with $x = 5$ and $y = 3$. Mass-selected laser photodissociation studies investigate the possible structural patterns in these novel complexes. Evidence is presented for multiple metal attachment on the same side of the coronene molecule, for metal and multimetal sandwich structures, and for multiple decker sandwich structures. Chromium atom insertion into the aromatic system is observed for several cluster sizes. Complexes with at least four chromium atoms fragment by extensive decomposition of the aromatic ring system.

Introduction

Metal π-complexes with various aromatic molecular ligands have fascinated organometallic chemists for many years.[1] Some of the earliest and best-known examples of these systems include ferrocene[2] and dibenzene chromium,[3] but there are now numerous other systems known. The diversity of metal π-complexes has increased dramatically in recent years with the development of gas phase cluster experiments where metal vapor can be combined directly with unusual ligand species in nontraditional synthetic schemes. For example, there are many experimental and theoretical studies of metal arene complexes.[4−12] Exohedral metallo-fullerenes[13−17] and metals bound to polycyclic aromatic hydrocarbons (PAH's)[18−25] have been described recently in molecular beam experiments and in mass spectrometry. Multidecker sandwiches and other network structures have been proposed for some of these systems. Although many of these new π-complex clusters have never been isolated, their structure and bonding properties are nonetheless interesting. In the present report, we investigate new examples of metal-PAH complexes in the form of chromium−coronene clusters.

Polycyclic aromatic hydrocarbons (PAHs) occur in many natural environments where carbon is present.[26] They are implicated in soot formation in hydrocarbon combustion and in the formation of dust grains in the interstellar medium. Theoretical models of metal intercalated graphite or carbon nanotube walls often employ PAH molecules as models representing a finite section of a carbon surface, but there is virtually no experimental data for the structures or energetics of metal attachment on these surfaces. Coronene ($C_{24}H_{12}$) is the smallest PAH having the essential structural elements of graphite. The optical properties of PAHs are well-studied including fluorescence and phosphorescence in the gas phase and in thin films.[27−30] Ionized PAHs have been implicated as carriers of the optical diffuse interstellar bands (DIBs)[31−34] or the unidentified infrared bands (UIRs).[35,36] Metal−PAH complexes have also been suggested to form in interstellar gas clouds.[18−20,37−41] Attachment to PAH surfaces is proposed to account for the depletion of certain metals (iron, magnesium, etc.) in the interstellar medium compared to their solar abundance. The spectroscopy and photochemistry of these systems are clearly of widespread interest.

Atomic metal ion complexes with selected PAH species (including coronene) have been described previously.[18−20] In recent laboratory work, our group has described the formation of metal and multimetal complexes of iron with coronene and other polyaromatic systems.[22,23] Competitive binding experiments with coronene, C_{60}, and benzene were used to establish a hierarchy of binding strengths to iron.[23] Additional experiments reported the formation of silver-coronene cation complexes[24] and vanadium−coronene anion complexes.[25] Coronene is particularly interesting for multimetal experiments because it is large enough to afford multiple binding sites for metal attachment on its surface. Interior or exterior rings are available for π-bonding on one or both sides of the organic surface. In the case of these iron−coronene complexes, photofragmentation processes suggest that iron forms a strong covalent bond with the PAH surface, that sandwich structures are quite stable, and that in multiple-metal complexes the iron binds as separated atoms on the coronene surface.[22] Chromium provides another reactive transition metal to investigate the possible generality of this kind of bonding. Because of the well-known stability of dibenzene chromium, we expect similar strong π-bonding of chromium with coronene and the possible formation of stable sandwich structures.

Experimental Section

Clusters for these experiments are produced by laser vaporization in a pulsed nozzle cluster source.[42] The sample for these experiments is a solid rod of chromium coated with a vapor-deposited thin film of coronene. The thin film was prepared via thermal evaporation of coronene in a separate sample preparation chamber and then the sample was transferred to the molecular beam experiment. Laser vaporization is accomplished with the focused output of a Nd:YAG laser (third harmonic, 355 nm) in a pulsed nozzle (Newport) source. The laser pulse energy is adjusted to penetrate through the organic film to ablate it and to vaporize the underlying metal so that both are produced in the gas phase. Cluster growth occurs in a 2 mm channel extending about 2 cm beyond the vaporization point. The

10.1021/jp002131s CCC: $19.00
Published on Web 11/05/2000

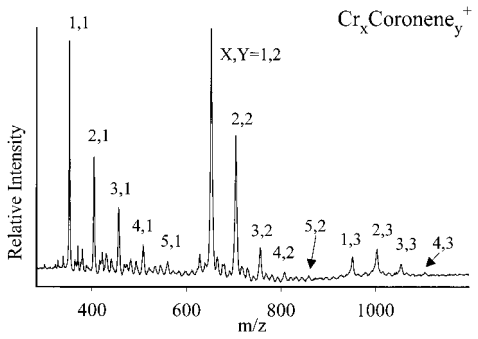

Figure 1. The mass distribution measured for $Cr_x-(coronene)_y^+$ ions produced by laser ablation/vaporization of a film-coated chromium rod.

positive ions produced directly from the laser vaporization plasma are sampled with a reflectron time-of-flight mass spectrometer with pulsed acceleration plate voltages.[42]

Mass-selected photodissociation experiments take place in the same reflectron time-of-flight mass spectrometer with the addition of a pulsed deflection plate (the so-called "mass-gate") which allows size selection of certain cluster masses. The operation of the instrument for these experiments has been described previously.[42] The time-of-flight through an initial drift tube section is used to size select the desired cluster, which is then excited with a pulsed laser (Nd:YAG; 532 or 355 nm) in the turning region of the reflectron field. The time-of-flight through the second drift tube section provides a mass spectrum of the selected parent ion and its photofragments, if any. The data are presented in a computer difference mode in which the dissociated fraction of the parent ion is plotted as a negative mass peak while its photofragments are plotted as positive peaks. Mass spectra are recorded with a digital oscilloscope (LeCroy) and transferred to a laboratory PC via an IEEE−488 interface.

Laser power and wavelength studies are employed to investigate the possibility of multiphoton processes and sequential fragmentation processes. The laser power required to photodissociate these molecules varies considerably with their size and stability. The highest laser power employed for any cluster represents the full intensity of the unfocused Nd:YAG laser harmonics (e.g., at 532 nm the pulse energy is perhaps 200 mJ in a 1.0 cm^2 spot size). This would be our limit of "extremely high power." "High power," as used below, indicates 50−100 mJ/cm^2, while low power refers to 1−10 mJ/cm^2.

Results and Discussion

Figure 1 shows the mass spectrum measured when cation clusters are grown by laser vaporization of a coronene-coated chromium rod. There is no ionization process other than recombination/growth in the plasma generated by the vaporization laser or growth via ion−molecule reactions in the channel extending beyond the vaporization region. The cations are extracted from the molecular beam with pulsed mass spectrometer acceleration voltages. As shown, a variety of $Cr_x(coronene)_y^+$ masses are produced. All the more intense peaks observed correspond to simple multiples of chromium and coronene, although there are some weaker masses which can be assigned to fragmentation of the coronene or to metal oxide adducts. The oxides come from surface impurities on the metal rod. Clusters are formed which contain up to five chromium atoms in complexes with one coronene molecule, up to five chromium atoms in complexes with two coronene molecules and up to four chromium atoms in complexes with three coronene molecules. For complexes with one or two coronene molecules, the most prominent mass peaks are those with a single chromium atom, and the intensities of multimetal complexes fall off gradually with size. This is approximately what would be expected from the metal density available for attachment. However, in complexes with three coronene molecules, there is a slightly enhanced abundance for the $Cr_2(coronene)_3$ stoichiometry which persists under a variety of mass spectrometer focusing conditions. This Cr:coronene 2:3 stoichiometry is the same as one of those seen by Kaya and coworkers for various metal−benzene clusters, which were suggested to have double-decker sandwich structures.[11] In the lower mass region (not shown) there are essentially no pure metal clusters. This suggests that the complexes here grow primarily as metal atoms are added one-by-one to the organic surface, rather than by the combination of clustered metal with the organic.

TABLE 1: The Ionization Potentials (IP) and Dissociation Energies (D_0) of Chromium and Its Small Clusters

species	IP (eV)	D_0 (cation)[a]	D_0 (neutral)
Cr	6.7665		
Cr_2	6.999[b]	1.30	1.54
Cr_3		2.01	
Cr_4		1.04	
Cr_5		2.34	

[a] Reference 44. [b] Reference 45.

This mass spectrum immediately raises questions about the structures of these clusters. In the multimetal adducts with a single coronene molecule, it is conceivable that the metal is clustered together in the form of an "island" on the surface of coronene. It is also conceivable that the metal is attached in smaller aggregates (atomic and/or molecular) at individual binding sites on the coronene molecular surface. Binding at η_5 or η_6 π sites is common in organometallic chemistry. Likewise, the metal in intercalated graphite occupies ring-centered sites.[43] However, the metal versus organic concentration here is higher than in those environments. The importance of clustered versus dispersed metal would then presumably depend on the relative strengths of metal−metal versus metal−organic bonding. It is conceivable that binding could occur on one or both sides of the coronene surface. The size of a chromium atom varies with its effective oxidation state, which is uncertain without some knowledge of the bonding in this system. However, reasonable estimates suggest that three chromium atoms in a film motif would cover one surface of a coronene molecule. Complexes with more than three metal atoms are therefore expected to have either metal clustered on metal or binding on both sides of the ring system. Having no convenient spectroscopic probe of these structures, we use mass-selected photodissociation experiments to investigate these various possibilities.

Table 1 shows the ionization potentials and bond energies for chromium clusters relevant for this work. Fortunately, the dissociation energies are known for chromium cluster cations up to several atoms in size from collision induced dissociation measurements.[44] Unfortunately, ionization energies are known for only the atom and the dimer.[45] Therefore, neutral bond energies cannot be derived for the larger cluster sizes. However, it is usually true that ionization energies decrease with size for metal clusters, and it is safe to assume that all chromium clusters will have ionization energies lower than that of coronene (7.29 eV). If this is true, then any pure chromium clusters eliminated by fragmentation will be charged and will therefore be observable with the mass spectrometer.

Figures 2−8 show various measurements of photodissociation mass spectra for clusters size selected from the distribution shown in Figure 1. These experiments use laser excitation with

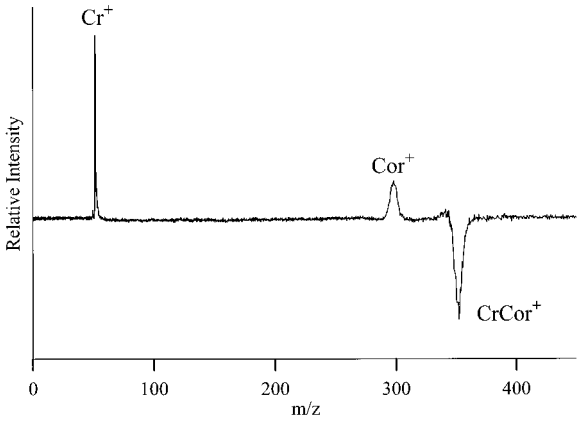

Figure 2. Photodissociation of the Cr−coronene$^+$ ion at 355 nm. Two apparent fragment ions are observed: Cr^+ and coronene$^+$. However, the coronene$^+$ ion signal has a steep dependence on the laser power and it is not observed at low power. It is therefore attributed to reionization of neutral coronene fragments.

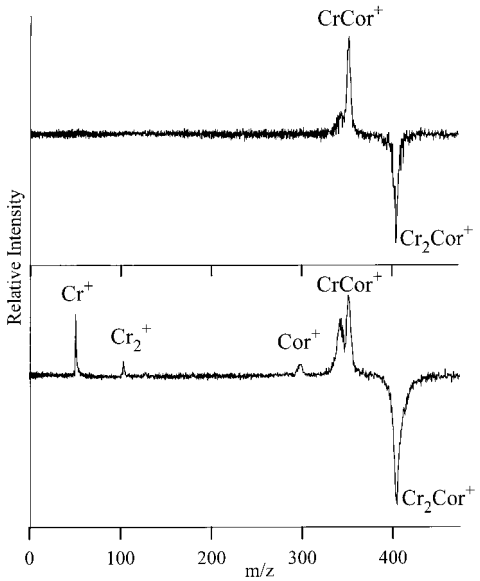

Figure 3. Photodissociation of Cr_2−coronene$^+$ at 355 nm. The upper trace is at the low power limit, which shows that the primary dissociation channel is loss of neutral chromium atoms. The shoulder at lower mass corresponds to loss of CrC. The lower trace is at high power, showing sequential fragmentation of Cr−coronene$^+$ and a parallel channel which produces Cr_2^+.

either the second (532 nm) or third (355 nm) harmonic of a Nd:YAG laser. At each wavelength for each cluster size, we vary the laser intensity to investigate the power dependence of the fragmentation processes and to see if there is sequential fragmentation. In all cases, we find that the power dependence varies with a high order in the laser fluence, i.e., the photodissociation processes are multiphoton. This is not unexpected. Coronene is a large enough molecule so that electronic excitation is expected to cause efficient internal conversion of energy to the ground electronic state, and the unimolecular rate of dissociation for such a large system should be quite slow. If metal is covalently attached to coronene, the metal-organic system is effectively coupled and the density of states for the combined complex is then greater than that for coronene itself. To dissociate such a system on the microsecond time scale of our instrument should require excitation well above threshold, and thus it is not surprising that multiphoton absorption is required to obtain measurable photodissociation in this experiment. Under these conditions it is difficult or impossible to

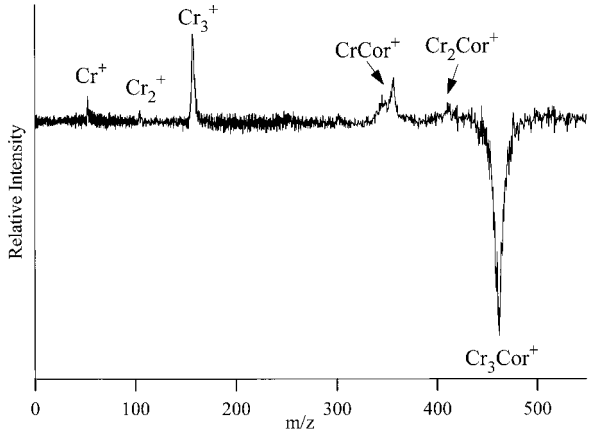

Figure 4. Photodissociation of Cr_3-coronene$^+$ at 355 nm. Two channels are suggested corresponding to sequential loss of chromium atoms and elimination of Cr_3^+.

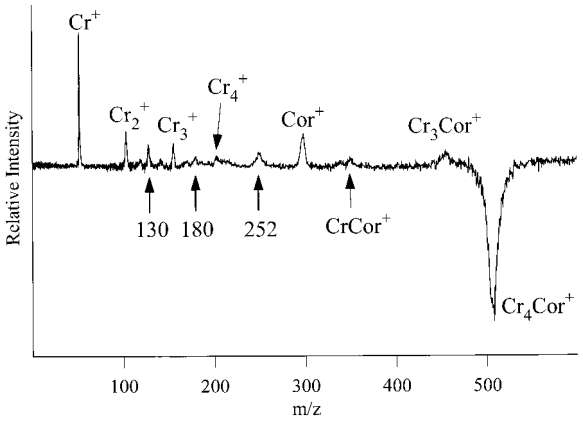

Figure 5. Photodissociation of Cr_4−coronene$^+$ at 355 nm.

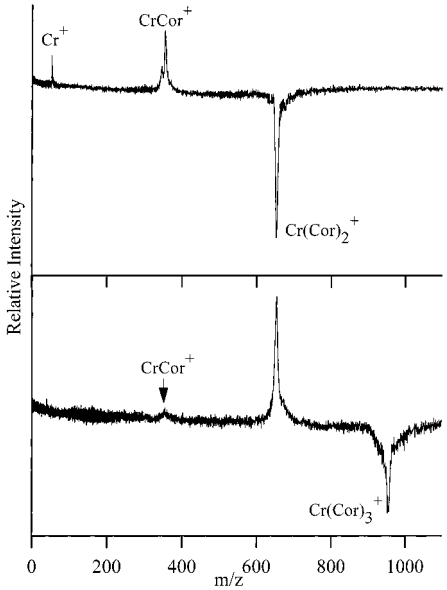

Figure 6. Photodissociation of Cr−(coronene)$_2^+$ and Cr−(coronene)$_3^+$ at 355 nm.

control the energy input into clusters, and therefore sequential fragmentation of primary photofragments often occurs. It is often not possible, then, to distinguish unequivocally between sequential and parallel fragmentation channels. We also note throughout the data that certain fragment peaks are broadened beyond the usual instrument resolution. This is understood to arise from metastable fragmentation of certain ions. Metastable

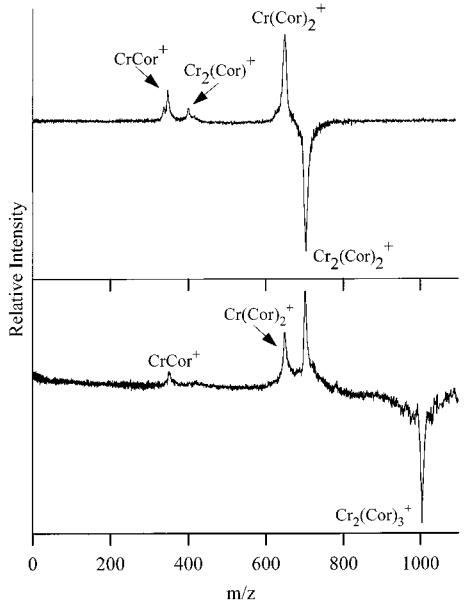

Figure 7. Photodissociation of $Cr_2-(coronene)_2^+$ and $Cr_2-(coronene)_3^+$ at 532 nm.

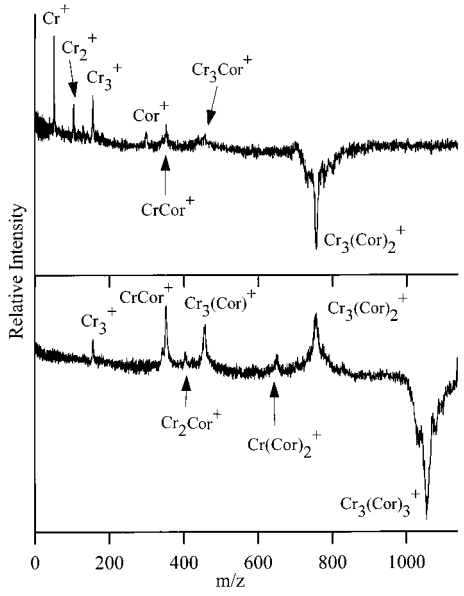

Figure 8. Photodissociation of $Cr_3-(coronene)_2^+$ and $Cr_3-(coronene)_3^+$ at 532 nm.

fragmentation, i.e., fragmentation on the time scale of acceleration out of the interaction region, may be found for large, stable ions with slow dissociation rates.

Figure 2 shows the photodissociation of the complex Cr−(coronene)$^+$. In this 1:1 complex, we see both chromium ion and coronene ion as fragments, which is somewhat surprising. We expect in such a simple metal−ligand cleavage that only the fragment with the lower ionization potential (IP) will be charged. Chromium has a lower IP (6.77 eV) than coronene (7.29 eV), and therefore we expect to see only Cr^+ in this process. However, the observation of the coronene ion as a fragment is possible if the photodissociation process accesses an excited state with "charge transfer" character. We have reported charge transfer photodissociation processes previously for a number of metal−benzene complexes.[7] The charge-transfer asymptote could be accessed if the excitation energy exceeds the metal−coronene IP difference (0.52 eV) and the (Cr−coronene)$^+$ bond energy, which is unknown. Unless the bound energy is quite high, then, it is not unreasonable that the laser energies here (532 nm, 2.33 eV; 355 nm, 3.49 eV) could accomplish this. However, laser power dependence studies show that this coronene cation channel is *not* produced via charge transfer. At low laser power (not shown), the coronene$^+$ fragment is not observed, and the only fragment ion is the expected Cr^+. This suggests that coronene is produced in the interaction region as a *neutral* photofragment, which then absorbs light in the intense laser field and becomes ionized via multiphoton absorption. Reionization of fragments is a common problem in systems like these which require high laser powers for fragmentation. This process is also seen below for larger chromium-coronene complexes.

Figure 3 shows the photodissociation of $Cr_2(coronene)^+$ at low (upper trace) and moderately high (lower trace) laser powers. At low power, the most prominent fragment is Cr−coronene$^+$, which is produced by the loss of neutral chromium atom. The observation of this charged fragment with the loss of neutral chromium suggests that Cr−coronene has a lower IP than that of Cr. There is also a lower mass shoulder at 340 amu. The resolution in the fragment spectrum is not high, but this peak can be assigned to a $Cr_2-coronene^+$ complex which has lost the fragment CrC. We see this same fragment ion as a satellite mass whenever Cr−coronene$^+$ is formed as a fragment ion from any larger cluster (see Figures 3−7). With our limited fragment ion resolution, we cannot rule out the additional loss of 1 or 2 hydrogen atoms. In any event, however, it is clear that there is a reactive channel in which metal has attacked the ring system and partially disrupted it. It is extremely unlikely that there would be a vacancy in one aromatic ring while a chromium atom is attached at another binding position. Therefore, it seems likely that this mass represents a chromium atom inserted into the coronene ring system. Insertion of niobium[46] and iron atoms[15e,16b] into the cage wall of C_{60} has been reported recently, and so this may represent an analogous process for coronene. At higher laser power in the lower trace, these two fragments are more prominent and additional fragment ions are observed. Again, there is a prominent atomic ion at low mass, which could come from sequential fragmentation of Cr−coronene$^+$. Likewise, the coronene peak could come from neutral coronene fragments from Cr−coronene$^+$ detected by reionization, as in Figure 2. However, a small amount of Cr_2^+ is detected, which cannot come from sequential fragmentation of Cr−coronene$^+$. It also cannot come from recombination of Cr and Cr^+ fragments because the density of parent ions is too low in the interaction region. Instead, this must represent a *parallel* channel of metal *dimer* elimination, which apparently has a lower cross section and can only be detected at higher power. This channel suggests that some fraction of the complexes present do not have inserted chromium, but instead have more weakly interacting metal.

Figure 4 shows the fragmentation of $Cr_3-coronene^+$ at moderate laser power (at 355 nm). The channels observed are similar to those seen before in that there is one sequence indicating the loss of one or two neutral atoms of chromium with the additional peak corresponding to CrC loss. Another channel represents the loss of Cr_3^+, where all the metal is eliminated at once. These again must represent parallel channels, which suggest that there are two different kinds of $Cr_3-coronene^+$ present. Presumably these fractions include one in which the metal is bound more tightly to the ring system (and perhaps inserted into it) and one in which metal is aggregated on the coronene surface but not as strongly attached to it. The dimer and atomic ions formed here have a laser power

dependence indicating that they come from fragmentation of Cr_3^+. In the limit of low laser power, Cr_3^+ is detected, but Cr_2^+ and Cr^+ are not. The observation of Cr_3^+ as a fragment ion here and Cr_2^+ as a fragment in Figure 3 suggests that the metal in these complexes is often, if not always, located on the same side of the coronene molecule. It is unlikely that metal bound on both sides could reassemble efficiently into clusters before elimination.

Figure 5 shows the photodissociation of Cr_4−coronene$^+$ at 355 nm. No ions with greater numbers of chromium atoms have a large enough signal for photodissociation. The signal here is weak, and high laser powers are necessary to measure any photodissociation. The photofragment with the highest mass is Cr_3−coronene$^+$, which appears as a broad feature consistent with metastable fragmentation. At lower masses, all the same fragments seen from Cr_3−coronene$^+$ are detected, perhaps by sequential fragmentation from this higher mass fragment ion. There is a small amount of Cr−coronene$^+$, but no Cr_2−coronene$^+$. The metastability of Cr_3−coronene and the low abundance of other possible Cr_x−coronene$^+$ fragments provides some suggestion that this three-atom complex is relatively stable. This is consistent with the geometric argument that three chromium atoms might fit nicely to cover one side of the ring system. More evidence for this effect is shown below. Other interesting fragments from this ion include a small amount of Cr_4^+. Unless there is a large rearrangement, this ion can only be formed from clusters which have all metal on the same side of the ring system. However, this mass may also correspond to an organometallic fragment, as shown below.

The surprising new features in this spectrum are fragment ions at 130, 180, and 252 amu, as well as a few other weaker peaks. These masses do not appear as prominent fragments from small complexes, and they cannot be assigned to any simple multiple of Cr and coronene. They must then correspond to organic or organometallic fragment ions in which the coronene ring system is dissociated. For example, mass 130 corresponds to Cr−benzene$^+$ and mass 180 corresponds to Cr−naphthalene$^+$. The broad peak at mass 252 corresponds approximately to Cr−pyrene$^+$, and this mass can be formed by elimination of Cr−(benzene)$_2$ (mass 208) from the parent ion. In all of these cases, the masses are uncertain by about 2 amu because of the peak widths and the resolution is not good enough to determine the presence or absence of 1 or 2 hydrogen atoms. Perhaps worth noting is that the peak indicated as Cr_4^+ occurs at a nominal mass of 208, which may also be assigned to Cr−(benzene)$_2^+$. Because of mass uncertainties, these peaks could also conceivably represent organic fragments without metal, e.g., naphthalene$^+$ ($M = 128$), tetracene$^+$ or phenanthracene$^+$ ($M = 178$), and perylene$^+$ ($M = 252$). However, metal-containing ions are more likely to be observed as charged species because of their lower ionization potentials. It is of course not unreasonable that an organometallic complex containing coronene should fragment to produce these smaller ring systems. Fragmentation of the coronene ring system is a relatively high energy process, and it is therefore also reasonable that extensive rearrangements might take place when this occurs. However, it is interesting that these fragments are not observed from complexes with fewer than four chromium atoms despite the extreme laser conditions used to initiate fragmentation. Apparently, the presence of at least four chromium atoms makes these new dissociation channels possible. Similar size effects requiring a certain number of adsorbed metal atoms for ring system decomposition have been observed previously in the photodissociation of metal−C_{60} complexes.[15]

Figure 6 shows the photodissociation of the Cr−(coronene)$_2^+$ and Cr−(coronene)$_3^+$ complexes at 532 nm. The strong intensity of the Cr−(coronene)$_2^+$ peak in the distribution of ions which grow from the cluster source suggests that it is relatively stable, and its stoichiometry naturally suggests that the structure might be a sandwich. This is also suggested because there are no pure coronene clusters evident in the source distribution. Apparently, chromium is necessary under these conditions to allow coronene to aggregate. In previous work, we have demonstrated the strong stability of Fe−(coronene)$_2^+$ complexes.[22] In the experiment here, we find again that only high power is sufficient to dissociate the 1,2 complex. The fragments seen include Cr−coronene$^+$ and the Cr^+ ion, as well as the 340 amu peak described earlier. The Cr−(coronene)$_3^+$ complex fragments primarily by loss of one coronene, to produce the Cr−(coronene)$_2^+$. These processes are consistent with a stable Cr−(coronene)$_2^+$ complex having a sandwich structure. In experiments not shown, we have added acetone as a reagent to probe the presence of exposed metal in these complexes. Cr_x−coronene$^+$ complexes, which must necessarily have exposed metal, all efficiently form adducts with one or two acetone molecules. However, Cr−(coronene)$_2^+$ does not form an acetone adduct under these same conditions. This result is also consistent with a sandwich structure having protected metal.

Figure 7 shows the fragmentation of the Cr_2−(coronene)$_2^+$ and Cr_2−(coronene)$_3^+$ ions. The most likely structures for Cr_2−(coronene)$_2^+$ are a metal dimer with surrounding coronene molecules (i.e., a sandwiched dimer) or any one of several possible structures for an atomic chromium sandwich with a metal atom added to the exterior (e.g., |●|●|). As indicated above, structures with clustered coronene and all-external metal are unlikely because there are no coronene clusters formed without metal under these conditions. The fragmentation pattern suggests that the structure with separated atoms is most likely. The highest mass fragment is Cr−(coronene)$_2^+$, which could correspond to loss of an external metal atom, while the other fragment ions match the higher mass fragments seen for Cr−(coronene)$_2^+$. The most likely fragment ion from a sandwiched dimer structure would be the loss of coronene and not the loss of metal. However, there is no evidence for Cr_2−coronene$^+$ or Cr_2^+ fragment ions. The data of Figures 2−4 suggest that metal cluster ions are formed when there is connected metal in the cluster. Therefore, the structure most consistent with the fragmentation pattern is a single atom sandwich with external metal. Consistent with this, when Cr_2−(coronene)$_2^+$ is exposed to acetone, it does form an acetone adduct suggesting that there is exposed metal.

The most likely structures for Cr_2−(coronene)$_3^+$ are a dimer surrounded by three coronene molecules or an alternating coronene−Cr−coronene−Cr−coronene (e.g., |●|●|) double sandwich. A dimer sandwich with external coronene is again unlikely because pure coronene clusters are not observed. Multiple sandwich structures have been suggested previously for V_x(benzene)$_y$ complexes and other multimetal organometallic complexes.[17] The fragmentation pattern here suggests that coronene is eliminated first, which would actually be expected for either of the possible structures. However, the lower mass fragments are essentially the same as those seen for Cr_2−(coronene)$_2^+$. Again, there are no fragments containing Cr_2^+. This suggests that there is an intermediate Cr_2−(coronene)$_2^+$ ion having the same structure as the ions fragmented above with this stoichiometry. If the intermediate is Cr_2−(coronene)$_2^+$ with the |●|● structure, then the best structure for Cr_2−(coronene)$_3^+$ is the double sandwich. This is definitely not structural proof,

but this structure provides the simplest explanation for the fragmentation pattern.

Figure 8 shows the fragmentation patterns for $Cr_3-(coronene)_2^+$ and $Cr_3-(coronene)_3^+$. For clusters this large, numerous isomeric structures are conceivable. However, the dissociation mass spectra contain only a few peaks. In the upper trace, the fragmentation of $Cr_3-(coronene)_2^+$ is shown. This cluster requires high power for dissociation, and the yield of photofragments is small. However, fragment ions may be detected at $Cr_3-coronene^+$, $Cr-coronene^+$, $coronene^+$, and Cr_3^+, Cr_2^+, Cr^+. There are no noticeable fragments for $Cr-(coronene)_2^+$ or $Cr_2-(coronene)_2^+$ which might be expected if the cluster is a one- or two-metal sandwich with external metal. Instead, the only fragment ion seen at high mass is a weak peak at Cr_3^+-coronene, which must come by the loss of coronene. The lower mass ions match the fragments of $Cr_3-coronene^+$ seen above in Figure 4. This suggests that this ion has a sandwich structure with three internal metal atoms, i.e., a *trimer* sandwich. A trimer sandwich was also suggested previously as a possible structure for $Fe_3-(coronene)_2^+$. The difficulty seen in fragmenting this ion suggests that it is quite stable.

The fragmentation of $Cr_3-(coronene)_3^+$, which has one more coronene, provides another probe of the stability and structure of $Cr_3-(coronene)_2^+$. If the latter is indeed a stable trimer sandwich, it might be expected as a prominent fragment from $Cr_3-(coronene)_3^+$, and indeed it is. $Cr_3-coronene^+$ and Cr_3^+ are prominent, which are exactly the fragments expected as a trimer sandwich breaks down. The other fragments are again essentially the same as those from $Cr_3-(coronene)_2^+$. The exceptions to this are a small amount of $Cr-(coronene)_2^+$ and Cr_2^+-coronene. These may also be fragments from $Cr_3-(coronene)_2^+$ that were just too weak to detect in the upper trace. So again, an ion which has many conceivable isomers has relatively few photofragments, and these are consistent with the loss of an extra coronene to produce a stable trimer $Cr_3-(coronene)_2^+$ sandwich.

Although fragmentation patterns do not determine structures or energetics directly, the consideration of these combined data allow several conclusions to be drawn about chromium−coronene complexes. The most obvious is that chromium forms strong bonding attachments to coronene. This is evident because all the complexes here require high power multiphoton conditions for fragmentation and because certain complexes undergo elimination of carbon or metal carbide fragments. In previous photodissociation studies of $Fe-(coronene)-R^+$ mixed sandwich clusters, where R = benzene or C_{60}, we showed that benzene or C_{60} are eliminated first and that coronene binds more strongly to iron than either of these other ligands.[23] Because the binding energy of $Fe-benzene^+$ is known (49 kcal/mol),[8] we were able to conclude that $Fe-coronene^+$ is bound by more than this. The binding of chromium with benzene is quite similar to that of iron (D_0 of $Cr-benzene^+ = 40$ kcal/mol).[8,9] Therefore, a strong binding of chromium with coronene is expected.

Another conclusion is that chromium atoms bind preferentially on the same side of the coronene ring. Although rearrangements are conceivable during fragmentation which would allow metal on opposite sides of the ring system to reassemble into a cluster, we see that there is almost always efficient formation of Cr_x^+ from $Cr_x-coronene^+$ ions. This suggests that a significant number of these complexes have metal on the same side. It is possible that chromium atoms form clusters in the gas phase first and then bind to coronene, which would also produce structures with contiguous metal. However, there are essentially no chromium clusters detected in the mass distribution from the source. In fact, as we described earlier for iron,[22] the source conditions and nozzle channel used here do not produce metal clusters efficiently when no organic is present. Therefore, we believe that these complexes grow by sequential addition of atoms to the organic. Apparently, the presence of metal on the organic molecular surface makes it more likely that an additional metal will stick and bind on that same side. Although there may be geometric and collisional cross section effects involved, it makes sense that open shell metal would bind effectively to open shell metal. Metal−metal bond energies are also significant, as shown in Table 1.

Closely related to the concept of preferential binding is the idea that there may be an activation energy associated with initial attachment of metal to the organic surface and perhaps again with insertion of metal into the ring system. A barrier to initial adsorption on the organic surface might explain why metal binds preferentially on faces with previously attached metal. Barriers to adsorption are not uncommon in surface science, and a barrier in these systems is also understandable in a qualitative sense. It is reasonable that the aromatic system would be disrupted in order to form π bonds, and that this could cause a barrier in the adsorption potential for attachment to the organic face. On the other hand, it is reasonable that there would be a lower barrier, if any, for attachment of metal to complexes with previously adsorbed metal. It is also reasonable that there would be another activation barrier for insertion of metal into the organic ring system. The experimental evidence for this is found in several systems (e.g., $Cr_2-coronene^+$ and $Cr_3-coronene^+$), where we see fragmentation via two parallel channels corresponding to different kinds of adsorbed metal. Some metal is strongly interacting with the organic (producing metal carbide fragments), and some metal is more weakly interacting (producing metal cluster fragments). Under the conditions in which these complexes grow, the temperature is initially quite hot when metal vapor has just been produced in the plasma, and then the clusters are cooled rapidly by supersonic expansion. It is reasonable that complexes which grow under the initial hot conditions might be better able to overcome a barrier to insertion into the ring system, while others that might grow later in the source would be cooler and would not be able to undergo insertion so efficiently. We also observe that a threshold number of four chromium atoms is necessary for fragmentation to produce extensive decomposition of the organic ring system. Although this mechanism may be quite complex, it may be that the complexes with more metal are better able to surmount a barrier to ring insertion.

The preferred site(s), if any, for metal attachment to the coronene ring system is also an interesting issue. While metal bonding in the central ring generates a structure with pleasing symmetry, it is actually more likely that such bonding will occur in the outer rings. Both NMR spectroscopy and theory find for example that there is greater electron density in the alternate outer rings of coronene.[47] Conventional synthetic chemistry has prepared complexes such as cyclopentadienyl−iron−coronene, in which binding occurs to these outer rings.[47−49] Likewise, ab initio calculations indicated that this kind of binding is favored.[20,37] If π-binding does occur in the electron-rich outer rings, then three metal atoms in alternate ring sites would cover a single side of coronene. A schematic of this is shown in Figure 9 as structure **a**).

The preferential binding of multiple metals to one side of coronene and the direction of binding at outer rings both have interesting implications for sandwich formation. It is then easy to see how a trimer sandwich might be formed. The exact

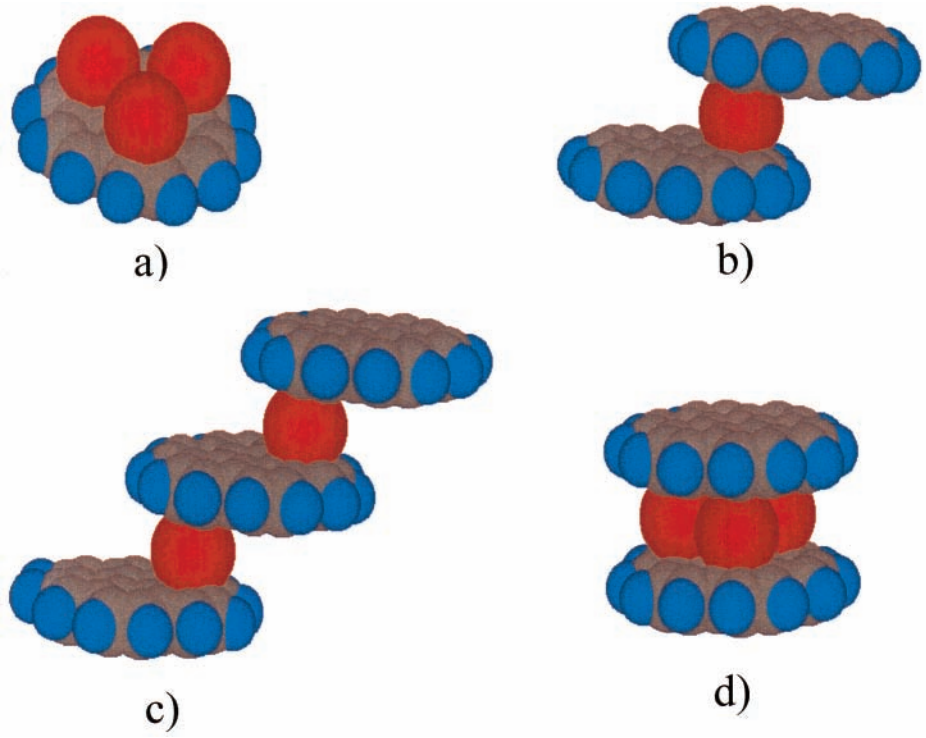

Figure 9. The structures proposed for various chromium-coronene complexes. In (**a**), the symmetric sites in which three chromium atoms can add to alternate rings on the same side of a single coronene system are shown. In (**b**), the staggered sandwich structure is shown. (**c**) shows the staggered double-decker sandwich, while (**d**) shows the symmetric three-metal sandwich.

registry between chromium atoms and alternate outside rings would favor aligned coronene molecules, and a highly symmetric structure would result, as shown in Figure 9, structure **d**). However, these tendencies would suggest surprising structures for sandwiches that have rings linked by single chromium atoms, e.g., the $Cr-(coronene)_2^+$ and $Cr_2-(coronene)_3^+$ species. The $Cr-(coronene)_2^+$ sandwich is then likely to adopt a structure with metal attachment to outer rings on both coronenes. Induction of charge in both ring systems would likely be caused by the metal binding, and the ends of the two coronenes opposite the metal would have similar polarity. This effect would then likely cause the two coronenes to rotate away from each other to form a staggered configuration, as shown in Figure 9, structure **b**). In a $Cr_2-(coronene)_3^+$ double-decker sandwich, then, continuation of this pattern would result in a "stair-step" conformation, as shown in Figure 9, structure **c**). However, while the fragmentation patterns provide some evidence that sandwich and double sandwich structures form, there is no information from these data about the specific conformations in these structures.

Much of the discussion so far implies that the coronene molecular structure retains its planarity in the formation of these complexes. This is indeed likely to be true for many complexes. However, there is nothing in these mass spectral data which allow this information to be determined. Quite the contrary, when there is a strong metal−organic interaction, such as the case of the Cr_4 complexes, it is not unreasonable that extensive rearrangement, including loss of ring planarity, may occur.

Conclusions

Chromium atoms are observed here to form strong attachments to the surface of coronene with the consequent growth of interesting cluster complexes. Complexes are formed with multiple atoms of chromium and with multiple coronene molecules. Evidence is presented that the binding of an initial chromium atom to coronene predisposes the complex to adsorption of additional metal atoms on this same side of the organic. In clusters which grow initially and in photofragments, there is a frequent occurrence of complexes with three chromium atoms, suggesting that this comprises a complete coverage of the coronene surface with a monolayer "film." A certain fraction of adsorbed chromium apparently forms a strong interaction with the coronene aromatic system, resulting in the formation of a complex with a chromium atom inserted into the ring system. Another fraction of the chromium is more weakly attached, and desorption produces pure metal clusters. However, the bonding energy for all complexes is significant, and multiphoton conditions are required for photodissociation. When at least four chromium atoms are attached to coronene, extensive fragmentation of the coronene molecule takes place producing a variety of organometallic fragment ions. Single chromium atoms combine with two coronene molecules in a sandwich structure analogous to the well-known complex dibenzene chromium. However, the structure for this is suggested to be staggered. The complex $Cr_2-(coronene)_3^+$ is suggested to be a double-decker sandwich, analogous to the $V_2-(benzene)_3$ clusters studied previously by Kaya and co-workers.[11] An additional remarkable sandwich is suggested which has three chromium atoms enclosed between two coronene molecules.

Taken together with previous observations on metal−coronene and other metal−PAH systems, these results suggest that metal−PAH binding and insertion chemistry represent fascinating new areas of organometallic bonding. These compounds appear to be extremely stable, and they may be accessible in macroscopic amounts via conventional (solution) or nonconventional (gas phase) synthetic schemes. Attempts in the latter area are underway in our laboratory. The bonding, structures, and energetics of these systems are largely unknown, and this should be a focus of future theoretical and spectroscopic studies. Photoelectron spectroscopy studies have recently been com-

pleted on the V_x−(coronene)$^-$ anions by our group in collaboration with the group of Kaya and co-workers.[50]

Acknowledgment. This research is supported by the Air Force Office of Scientific Research through Grant F49620-00-1-0118 and F49620-97-1-0386, and by the National Science Foundation through Grant CHE-9983580.

References and Notes

(1) Abel, E. W.; Stone, F. G. A.; Wilkinson, G. *Comprehensive Organometallic Chemistry II*; Pergamon Press: Oxford, 1994.

(2) Kealy, T. J.; Paulson, P. L. *Nature* **1951**, *168*, 1039.

(3) Fischer, E. O.; Hafner, W. *Z. Naturforsch.* **1955**, *10B*, 665.

(4) a) Ma, J. C.; Dougherty, D. A. *Chem. Rev.* **1997**, *97*, 1303. (b) Dougherty, D. A. *Science* **1996**, *271*, 163.

(5) Caldwell, J. W.; Kollman, P. A. *J. Am. Chem. Soc.* **1995**, *117*, 4177.

(6) a) Jacobson, D. B.; Freiser, B. S. *J. Am. Chem. Soc.* **1984**, *106*, 3900. (b) Jacobson, D. B.; Freiser, B. S. *J. Am. Chem. Soc.* **1984**, *106*, 4623. (c) Rufus, D.; Ranatunga, A.; Freiser, B. S. *Chem. Phys. Lett.* **1995**, *233*, 319. (d) Afzaal, S.; Freiser, B. S. *Chem. Phys. Lett.* **1994**, *218*, 254.

(7) a) Willey, K. F.; Cheng, P. Y.; Bishop, M. B.; Duncan, M. A. *J. Am. Chem. Soc.* **1991**, *113*, 4721. (b) Willey, K. F.; Yeh, C. S.; Robbins, D. L.; Duncan, M. A. *J. Phys. Chem.* **1992**, *96*, 9106.

(8) a) Chen, Y. M.; Armentrout, P. B. *Chem. Phys. Lett.* **1993**, *210*, 123. (b) Meyer, F.; Khan, F. A.; Armentrout, P. B. *J. Am. Chem. Soc.* **1995**, *117*, 9740.

(9) a) Sodupe, M.; Bauschlicher, C. W. *J. Phys. Chem.* **1991**, *95*, 8640. (b) Sodupe, M.; Bauschlicher, C. W.; Langhoff, S. R.; Partridge, H. *J. Phys. Chem.* **1992**, *96*, 2118. (c) Bauschlicher, C. W.; Partridge, H.; Langhoff, S. R. *J. Phys. Chem.* **1992**, *96*, 3273. (d) Sodupe, M.; Bauschlicher, C. W. *Chem. Phys.* **1994**, *185*, 163.

(10) (a) Dunbar, R. C.; Klippenstein, S. J.; Hrusak, J.; Stöckigt, D.; Schwartz, H. *J. Am. Chem. Soc.* **1996**, *118*, 5277. (b) Ho, Y. P.; Yang, Y. C.; Klippenstein, S. J.; Dunbar, R. C. *J. Phys. Chem.* **1997**, *101*, 3338.

(11) (a) Hoshino, K.; Kurikawa, T.; Takeda, H.; Nakajima, A.; Kaya, K. *J. Phys. Chem.* **1995**, *99*, 3053. (b) Judai, K.; Hirano, M.; Kawamata, H.; Yabushita, S.; Nakajima, A.; Kaya, K. *Chem. Phys. Lett.* **1997**, *270*, 23. (c) Nagao, S.; Negishi, Y.; Kato, A.; Nakamura, Y.; Nakajima, A.; Kaya, K. *J. Phys. Chem. A* **1999**, *103*, 8909.

(12) a) Roth, L. M.; Huang, Y.; Schwedler, J. T.; Cassady, C. J.; Ben-Amotz, D.; Kahr, B.; Freiser, B. S. *J. Am. Chem. Soc.* **1991**, *113*, 6298. (b) Huang, Y.; Freiser, B. S. *J. Am. Chem. Soc.* **1991**, *113*, 8186. (c) Huang, Y.; Freiser, B. S. *J. Am. Chem. Soc.* **1991**, *113*, 9418. (d) Jiao, Q.; Huang, Y.; Lee, S. A.; Gord, J. R.; Freiser, B. S. *J. Am. Chem. Soc.* **1992**, *114*, 2726.

(13) Basir, Y.; Anderson, S. L, *Chem. Phys. Lett.* **1995**, *243*, 45.

(14) Welling, M.; Thompson, R. I.; Walther, H. *Chem. Phys. Lett.* **1996**, *253*, 37.

(15) (a) Martin, T. P.; Malinowski, N.; Zimmermann, U.; Naher, U.; Schaber, H. J. *J. Chem. Phys.* **1993**, *99*, 4210. (b) Zimmermann, U.; Malinowski, N.; Naher, U.; Frank, S.; Martin, T. P. *Phys. Rev. Lett.* **1994**, *72*, 3542. (c) Tast, F.; Malinowski, N.; Frank, S.; Heinebrodt, M.; Billas, I. M. L.; Martin, T. P. *Phys. Rev. Lett.* 77 1996 3529. (d) Tast, F.; Malinowski, N.; Billas, I. M. L.; Heinebrodt, M.; Martin, T. P. *Z. Phys. D: At., Mol. Clusters* **1997**, *40*, 351. (e) Branz, W.; Billas, I. M. L.; Malinowski, N.; Tast, F.; Heinebrodt, M.; Martin, T. P. *J. Chem. Phys.* **1998**, *109*, 3425.

(16) (a) Reddic, J. E.; Robinson, J. C.; Duncan, M. A. *Chem. Phys. Lett.* **1997**, *279*, 203. (b) Grieves, G. A.; Buchanan, J. W.; Reddic, J. E.; Duncan, M. A. *Int. J. Mass Spectrom.* **2000**. In press.

(17) (a) Nakajima, A.; Nagao, S.; Takeda, H.; Kurikawa, T.; Kaya, K. *J. Chem. Phys.* **1997**, *107*, 6491. (b) Kurikawa, T.; Nagao, S.; Miyajima, K.; Nakajima, A.; Kaya, K. *J. Phys. Chem. A* **1998**, *102*, 1743. (c) Nagao, S.; Kurikawa, T.; Miyajima, K.; Nakajima, A.; Kaya, K. *J. Phys. Chem. A* **1998**, *102*, 4495. (d) Nagao, S.; Negishi, Y.; Kato, A.; Nakamura, A.; Nakajima, A.; Kaya, K. *J. Phys. Chem. A* **1999**, *103*, 8909. (e) Nakajima, A.; Kaya, K. *J. Phys. Chem. A* **2000**, *104*, 176.

(18) Marty, P.; de Parseval, P.; Klotz, A.; Chaudret, B.; Serra, G.; Boissel, P. *Chem. Phys. Lett.* **1996**, *256*, 669.

(19) Marty, P.; de Parseval, P.; Klotz, A.; Serra, G.; Boissel, P. *Astron. Astrophys.* **1996**, *316*, 270.

(20) Klotz, A.; Marty, P.; Boissel, P.; de Caro, D.; Serra, G.; Mascetti, J.; de Parseval, P.; Deroualt, J.; Daudey, J.-P.; Chaudret, B. *Planet. Space Sci.* **1996**, *44*, 957.

(21) Pozniak, B. P.; Dunbar, R. C. *J. Am. Chem. Soc.* **1997**, *119*, 10439.

(22) Buchanan, J. W.; Reddic, J. E.; Grieves, G. A.; Duncan, M. A. *J. Phys. Chem. A* **1998**, *102*, 6390.

(23) Buchanan, J. W.; Grieves, G. A.; Reddic, J. E.; Duncan, M. A. *Int. J. Mass Spectrom.* **1999**, *182/183*, 323.

(24) Buchanan, J. W.; Grieves, G. A.; Flynn, N. D.; Duncan, M. A. *Int. J. Mass Spectrom.* **1999**, *185*−*187*, 617.

(25) Duncan, M. A.; Knight, A. M.; Negishi, Y.; Nagao, S.; Nakamura, Y.; Kato, A.; Nakajima, A.; Kaya, K. *Chem. Phys. Lett.* **1999**, *309*, 49.

(26) Harvey, R. G. *Polyaromatic Hydrocarbons*; Wiley-VCH: New York, 1996.

(27) Birks, J. B. *Photophysics of Aromatic Molecules*: John Wiley: London, 1970.

(28) Klessinger, M.; Michl, J. *Excited States and Photochemistry of Organic Molecules*; VCH Publishers: New York, 1995.

(29) Karcher, W.; Fordham, R. J.; Dubois, J. J.; Glaude, P. G. J. M.; Lighthart, J. A. M., Eds. *Spectral Atlas of Polyaromatic Hydrocarbons*; D. Reidel Publishers: Dordrecht, 1985.

(30) Babbitt, R. J.; Ho, C.-J.; Topp, M. R. *J. Phys. Chem.* **1988**, *92*, 2422.

(31) Bohme, D. K. *Chem. Rev.* **1992**, *92*, 1487.

(32) Tielens, A. G. G. M.; Snow, T. P. Eds., *The Diffuse Interstellar Bands*; Kluwer Academic Publishers: Dordrecht, 1995.

(33) Salama, F.; Bakes, E. L. O.; Allamandola, L. J.; Tielens, A. G. G. M. *Astrophys. J.* **1996**, *458*, 621.

(34) Henning, T.; Salama, F. *Science* **1998**, *282*, 2204.

(35) Allamandola, L. J.; Tielens, A. G. G. M.; Barker, J. R. *Astrophys. J. Supp.* **1989**, *71*, 733.

(36) Léger, A.; d'Hendecourt, L.; Défourneau, D. *Astron. Astrophys.* **1989**, *216*, 148.

(37) Chaudret, B.; Le Beuze, A.; Rabaâ, H.; Saillard, J. Y.; Serra, G. *New J. Chem.* **1991**, *15*, 791.

(38) Serra, G.; Chaudret, B.; Saillard, J.-Y et al. *Astron. Astrophys.* **1992**, *260*, 489.

(39) Marty, P.; Serra, G.; Chaudret, B.; Ristorelli, I. *Astron. Astrophys.* **1994**, *282*, 916.

(40) Ristorelli, I.; Klotz, A. *Astron. Astrophys.* **1997**, *317*, 962.

(41) Klotz, A.; Marty, P.; Boissel, P.; Chaudret, B.; Daudey, J. P. *Astron. Astrophys.* **1995**, *304*, 520.

(42) Yeh, C. S.; Pilgrim, J. S.; Robbins, D. L.; Willey, K. F.; Duncan, M. A. *Int. Rev. Phys. Chem.* **1994**, *13*, 231.

(43) Müller, U. *Inorganic Structural Chemistry*; John Wiley: Chichester, 1993.

(44) Armentrout, P. B.; Hales, D. A.; Lian, L. *Advances in Metal & Semiconductor Clusters*; Duncan, M. A., Ed.; JAI Press: Greenwich, CT, 1994; Vol. 2, p 1.

(45) Simard, B.; Lebeault-Dorget, M.-A.; Marijnissen, A.; ter Meulen, J. J. *J. Chem. Phys.* **1998**, *108*, 9668.

(46) Clemmer, D. E.; Hunter, J. M.; Shelimov, K. B.; Jarrold, M. F. *Nature* **1994**, *372*, 248.

(47) Schmitt, G.; Kein, W.; Fleischhauer, J.; Walbergs, U. *J. Organomet. Chem.* **1978**, *152*, 315.

(48) Morrison, W. H.; Ho, E. Y.; Hendrickson, D. N. *Inorg. Chem.* **1975**, *14*, 500.

(49) Astruc, D. *Tetrahedron* **1983**, *39*, 4027.

(50) Duncan, M. A.; Knight, A. M.; Negishi, Y.; Nagao, S.; Nakamura, Y.; Kato, A.; Nakajima, A.; Kaya, K. To be submitted. *Corresponding author. E-mail: maduncan@arches.uga.edu.